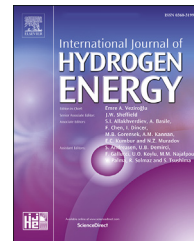




ELSEVIER

Available online at [www.sciencedirect.com](http://www.sciencedirect.com)

ScienceDirect

journal homepage: [www.elsevier.com/locate/he](http://www.elsevier.com/locate/he)

# MOF-derived NiSe<sub>2</sub> nanoparticles grown on carbon fiber as a binder-free and efficient catalyst for hydrogen evolution reaction

Ha Huu Do <sup>a</sup>, Chinh Chien Nguyen <sup>b,c</sup>, Dang Le Tri Nguyen <sup>d,e</sup>,  
Sang Hyun Ahn <sup>a</sup>, Soo Young Kim <sup>f,\*\*</sup>, Quyet Van Le <sup>b,\*</sup>

<sup>a</sup> School of Chemical Engineering and Materials Science, Chung-Ang University, 84 Heukseok-ro, Dongjak-gu, Seoul, 06974, Republic of Korea

<sup>b</sup> Institute of Research and Development, Duy Tan University, Da Nang 550000, Viet Nam

<sup>c</sup> Faculty of Environmental Chemical Engineering, Duy Tan University, Da Nang 550000, Viet Nam

<sup>d</sup> Division of Computational Physics, Institute for Computational Science, Ton Duc Thang University, Ho Chi Minh City, Viet Nam

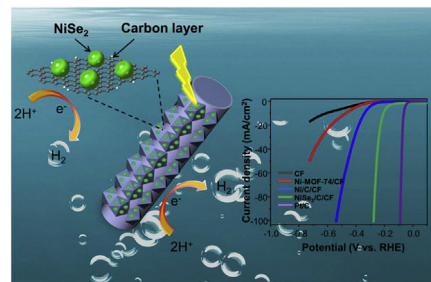
<sup>e</sup> Faculty of Applied Sciences, Ton Duc Thang University, Ho Chi Minh City, Viet Nam

<sup>f</sup> Department of Materials Science and Engineering, Korea University, 145 Anam-ro Seongbuk-gu, Seoul 02841, Republic of Korea

## HIGHLIGHTS

- Approach for the preparation of low-cost and stable catalysts for HER was introduced.
- Binder-free catalyst for HER based on MOF-derived NiSe<sub>2</sub>/C/CF was constructed.
- NiSe<sub>2</sub>/C/CF gives a low overpotential of 209 mV, a Tafel slope of 74.1 mV/dec.
- NiSe<sub>2</sub>/C/CF catalyst exhibits excellent stability under working condition.

## GRAPHICAL ABSTRACT



## ARTICLE INFO

### Article history:

Received 13 February 2022

Received in revised form

30 March 2022

Accepted 14 April 2022

Available online xxx

## ABSTRACT

It is challenging to grow inexpensive cathode material with superior catalytic properties for hydrogen evolution reaction (HER). Metal-organic frameworks (MOFs) have emerged as powerful platforms to synthesize efficient and ultrastable catalysts for hydrogen production. In this research, NiSe<sub>2</sub> nanoparticles were derived from Ni-based MOF, which grown in situ on carbon fiber (NiSe<sub>2</sub>/C/CF) through pyrolysis and selenization processes. NiSe<sub>2</sub>/C/CF displays a higher HER performance than that of Ni/C/CF and Ni-MOF-74/CF. Notably, the NiSe<sub>2</sub>/C/CF electrode gives a low overpotential of 209 mV, a Tafel slope of 74.1 mV/dec, and

\* Corresponding author.

\*\* Corresponding author.

E-mail addresses: [nguyenletridang@tdtu.edu.vn](mailto:nguyenletridang@tdtu.edu.vn) (D.L.T. Nguyen), [sooyoungkim@korea.ac.kr](mailto:sooyoungkim@korea.ac.kr) (S.Y. Kim), [levanquyet@tdtu.edu.vn](mailto:levanquyet@tdtu.edu.vn), [quyetbk88@korea.ac.kr](mailto:quyetbk88@korea.ac.kr) (Q.V. Le).

<https://doi.org/10.1016/j.ijhydene.2022.04.127>

0360-3199/© 2022 Hydrogen Energy Publications LLC. Published by Elsevier Ltd. All rights reserved.

**Keywords:**

Metal-organic frameworks  
Carbon fiber  
Nickel diselenide  
Hydrogen evolution reaction

outstanding stability with slight decay after operating for 12 h. The high HER catalytic activity of NiSe<sub>2</sub>/C/CF is mainly ascribed to the emerging effects of NiSe<sub>2</sub> nanoparticles and three-dimensional conductive substrate CF, facilitating active moieties exposure and electron transfer during the electrocatalytic process. Therefore, this work illustrates a novel approach for the preparation of transition metal chalcogenides as low-cost and stable catalysts for HER.

© 2022 Hydrogen Energy Publications LLC. Published by Elsevier Ltd. All rights reserved.

## Introduction

Electrochemical water splitting is a straightforward method to produce hydrogen, which plays an essential role in addressing the issue of clean energy. However, the main disadvantage of water dissociation is that applied overvoltage is required high to surpass the energy barrier for hydrogen evolution reactions (HER). To date, noble metals (e.g., Pt, Pd, Rh) were proved to be the best materials to prepare cathode for electrochemical HER [1]. However, the high-priced of these catalysts inhibited a wide range of industrial processes. A large number of works were carried out to find non-noble metal-related electrocatalysts, such as transition metal oxides [2–5], sulfides [6–9], carbides [10–14], and selenides [15–17] for hydrogen-evolving. In this regard, nickel diselenide has gained growing attention as a potential rival to alter noble metal catalysts by its intrinsically good catalytic activity, outstanding durability, and low production cost [18–20]. However, bulk NiSe<sub>2</sub> has low active species, poor conductivity, which is not favorable for electrocatalytic utilizations [21–23]. Its HER activity thus needs to be boosted to become commercial catalysts. Numerous studies have attempted to enhance the HER performance of NiSe<sub>2</sub> via various approaches such as designing nanoarchitecture or employing conductive templates. For example, Li et al. prepared NiSe<sub>2</sub> nanoparticles with supporting nitrogen-doped graphene toward enhanced HER performance [18]. Nickel foam with a three-dimensional (3D) architecture was evaluated as an ideal skeleton for growth materials to create efficient electrodes for electrochemical applications [24–26]. As a case in point, Zhou et al. create NiSe<sub>2</sub> on a nickel foam (NF) platform as an efficient electrode for hydrogen evolving, which is assigned to the emerging effect of catalytic species exposure and fast electron transfer from the high conductivity of NF. This electrode gave an excellent HER catalytic property, which is comparable to Pt/C catalysts. In a similar case in Teng's work, the authors synthesized NiSe<sub>2</sub> nanotube arrays on NF as a functional cathode for water dissociation [27]. The effectiveness of NF substrate has been exemplified in a study by Yu and coworkers [28]. However, the drawback of NF is not durable at high temperatures, which is usually used for fabrication catalyst materials [29]. Also, carbon fiber (CF) is employed as a conductive substrate to prepare electrodes in catalytic utilization because of its superior properties, including good chemical stability, high thermal stability, large surface area, and outstanding

mechanical strength [30–33]. For instance, Qu et al. deposited MoSe<sub>2</sub> nanosheets CF as a 3D cathode for hydrogen evolution [34]. This cathode gave an excellent catalyst with a low overvoltage, which was ascribed to the synergistic engineering of nanosheets and a highly conductive template. Hou and co-workers fabricated Pt/MoS<sub>2</sub>/CF as a working electrode for HER in an acidic solution, which exhibited remarkable stability with 10 h of operation [35]. Zang et al. used carbon fiber felt (CFF) to grow MoS<sub>2</sub> nanolayers as a flexible electrode with outstanding HER activity [36]. Zhang et al. found that the in situ synthesis of MoS<sub>2</sub> on carbon cloth (CC) created an electrocatalyst with better performance than the physical preparation of MoS<sub>2</sub> with CC [37]. Wang et al. also used CC as a 3D conductive platform to deposit CoSe<sub>2</sub> nanocatalysts anchored Co–N-doped carbon matrix for HER [38]. This catalyst displayed a very low Tafel slope comparable with Pt catalyst for hydrogen production. Another work that utilized CC for growth cobalt disulfide nanotube arrays were reported by Guan et al. [39]. The authors found that this material exhibited higher stability than Pt/C catalyst for HER application. Yan and co-workers have confirmed the effectiveness of the CC template [40]. The authors synthesized WS<sub>2</sub> and MoS<sub>2</sub> on CC through a facial solvothermal process. The electrodes display remarkable durability after 24 h of testing, which is attributed to the good interaction between materials and CC. As mentioned pieces of evidence, the carbon-based substrates' role is significant for preparing efficient, binder-free, and durable electrodes in electrochemical HER. The metal-organic framework was considered ideal for creating unique architecture with high performance in catalysis because of its outstanding properties, such as large surface area and adjustable structural morphology. However, MOFs-derived materials are usually created with powder catalysts, which must use binders (Nafion, polytetrafluoroethylene) to fabricate the working electrodes [41]. This may affect the catalytic activity in the electrochemical reaction, impeding their commercial utilization. Therefore, researchers synthesized the MOFs on conductive substrates, then converted them to nanocatalysts anchored on this template for water dissociation. For example, Wang and coworkers prepared CoSe<sub>2</sub> nanoparticles from Co-based MOF nanosheets on CF, which gave an excellent catalytic activity with a Tafel slope of 38 mV/dec [38]. The effectiveness of CF has been proved in a report by Zhan et al. [42]. The authors grow Co-MOF on CF through an active binder carbon nanotube, followed by the oxidation and phosphorization to form CoP nanograins as a highly stable

electrocatalyst for hydrogen generation. Xie et al. fabricated Ni-doped CoS<sub>2</sub> on carbon fiber papers (CFP) as efficient catalysts for oxygen evolution reaction with an overvoltage of 270 mV [43]. Beside Co-MOF, Ni-based MOFs were also used to create Ni compounds for HER. However, the in situ synthesis of Ni-MOF-74 on CF as precursor for preparation NiSe<sub>2</sub> has not investigated yet for HER application.

In this study, we introduce a straightforward approach to fabricating NiSe<sub>2</sub> nanoparticles from Ni-based MOF, grown in situ on commercial carbon fiber (NiSe<sub>2</sub>/C/CF) as a binder-free and efficient cathode for hydrogen production in acidic media. NiSe<sub>2</sub>/C/CF exhibits an outstanding catalytic activity with a slight overvoltage of 209 mV at a current density of 10 mA/cm<sup>2</sup> and a low Tafel slope of 74.1 mV/dec. Also, this electrode displays remarkable durability, remaining catalytic properties after 10 h. The high performance of NiSe<sub>2</sub>/C/CF is ascribed to the emerging effects of a conductive substrate and highly active sites of NiSe<sub>2</sub> nanoparticles.

## Experimental section

### Materials

Phychemi company provided carbon fiber. Nickel nitrate hexahydrate, Nafion media (5 wt %), 2,5-Dihydroxybenzenedicarboxylic acid (H<sub>4</sub>DHBDC), Selene powder were supplied from Sigma-Aldrich. N,N-Dimethylformamide (DMF), Ethanol (C<sub>2</sub>H<sub>5</sub>OH), Sulfuric acid (98%) were bought from Daejung Chemicals & Metals Company Limited. The water utilized in experimental studies was obtained from an instrument of Millipore Mili-Q.

### Synthesis of Ni-MOF-74/CF

The pristine CF (2 cm × 3 cm) was oxidized in air at 450 °C for 30 min to increase the hydrophilic properties for its surface, which is favorable for the growth of MOF crystals. Then, it was rinsed with DI water and ethanol for 15 min. Next, the reaction solution was fabricated by dissolving 0.238 g of Ni(NO<sub>3</sub>)<sub>2</sub>·6H<sub>2</sub>O and 0.048 g of H<sub>4</sub>DHBDC in a mixture solvent (5 ml DMF, 5 ml DI water, 5 ml ethanol). The modified CF was immersed into this reaction solution and heated at 100 °C for 24 h. Finally, the as-prepared Ni-MOF-74/CF was washed with ethanol, accompanied by drying under vacuum at 80 °C for 5 h.

### Synthesis of NiSe<sub>2</sub>/C/CF

The sample of NiSe<sub>2</sub>/C/CF was obtained over two steps of calcination and selenization. Firstly, the as-prepared Ni-MOF-74/CF was pyrolyzed at 500 °C for 2 h in nitrogen gas to produce Ni/C/CF. Second, a sample of Ni/C/CF was conducted selenization to create NiSe<sub>2</sub>/C/CF. In particular, a piece of Ni/C/CF is put in a combustion boat with 50 mg of Se powder at the upstream side, followed by reacting at 350 °C for 2 h under a nitrogen atmosphere. The mass loading of NiSe<sub>2</sub>/C on CF is approximately 1.0 mg/cm<sup>2</sup> determined by the mass change between CF and NiSe<sub>2</sub>/C/CF.

## Characterization

A SIGMA/Carl Zeiss microscope was chosen to obtain scanning electron microscopy (SEM) images. JEOL-2100F (Japan) electron microscope are adopted for collecting Transmission electron microscopy (TEM) and high-resolution TEM (HRTEM) images. X-ray diffraction (XRD) data are collected on a D8-Advance/Bruker-AXS with Cu K $\alpha$  radiation. The chemical states of elements in materials were investigated by X-ray photoelectron spectroscopy (XPS). The Raman spectra data were gathered on a Raman microscope (LabRAM-HR) in a frequency zone of 100–3500 cm<sup>-1</sup>.

### Measurements of electrochemical properties

The HER catalytic activities of the catalysts were judged in the electrolyte of 0.5 M H<sub>2</sub>SO<sub>4</sub> with a potentiostat workstation (Ivium 5612). Carbon rod, Hg/Hg<sub>2</sub>Cl<sub>2</sub> in KCl (saturated), and as-prepared electrodes (working area of 1.0 cm × 1.0 cm) operated as an auxiliary, reference, and working electrodes. Herein, voltages vs. reversible hydrogen electrode (RHE) are determined from the Nernst equation of E (RHE) = E (Hg/Hg<sub>2</sub>Cl<sub>2</sub>) + 0.059 × pH + 0.241. Polarization curves are recorded in a voltage range of -0.08–0.1 (vs. RHE) at a scan rate of 10 mV/s, followed by iR correction. Electrochemical impedance spectroscopy (EIS) plots were gathered in frequencies zone of 0.1 Hz–100 kHz. The durable properties of the working electrode were evaluated by utilizing cyclic voltammetry (CV) in a potential window from 0.1 to -0.3 V (RHE) at a scan rate of 100 mV/s and chronoamperometry for up to 12 h at a constant voltage.

## Result and discussion

The synthetic route of nickel diselenides from Ni-based MOF grown on CF is exhibited in Fig. 1. First, Ni-MOF-74 was in situ synthesized on CF (abbreviated Ni-MOF-74/CF) by solvent-thermal method; then it is converted into Ni nanoparticles embedded on carbon layers (Ni/C/CF) at 500 °C, followed by selenization to form NiSe<sub>2</sub> nanograins anchored carbon layer array on CF (NiSe<sub>2</sub>/C/CF). The crystal architectures of CF, Ni-MOF-74/CF, Ni/C/CF, NiSe<sub>2</sub>/C/CF samples were investigated by XRD spectroscopy (Fig. 2a). A typical peak of CF was identified at about 24.5° indexed to (002) planes, which was appeared in all samples [30]. Two diffraction peaks at 6.8° and 11.7° were observed in the Ni-MOF-74/CF sample that proved the successful growth of Ni-MOF-74 on CF [44–46]. The three peaks of 44.2°, 51.5°, and 75.8° were assigned to the (111), (200), and (220) planes of metallic Ni [19,47], which implied the complete conversion of Ni-MOF-74/CF into Ni/C/CF. The XRD pattern of NiSe<sub>2</sub>/C/CF exhibits the peaks at 2θ values of 29.9°, 33.4°, 36.7°, 42.6°, 50.5°, 55.2° and 57.5° which were attributed to the (200), (210), (211), (220), (311), (230) and (321) planes (PDF# 88–1711) [20]. Fig. 2b exhibits the Raman spectra peaks of NiSe<sub>2</sub>/C/CF. Signal frequencies of 149.6, 169.9, 217.5, and 243.7 cm<sup>-1</sup> are indexed to the T<sub>g</sub>, F<sub>g</sub>, A<sub>g</sub>, and T<sub>g</sub> modes of NiSe<sub>2</sub> [27]. The high-intensity peaks at 1357, 1590, and 2709 cm<sup>-1</sup> correspond to the D-, G-, and 2D-band of carbon materials [48].

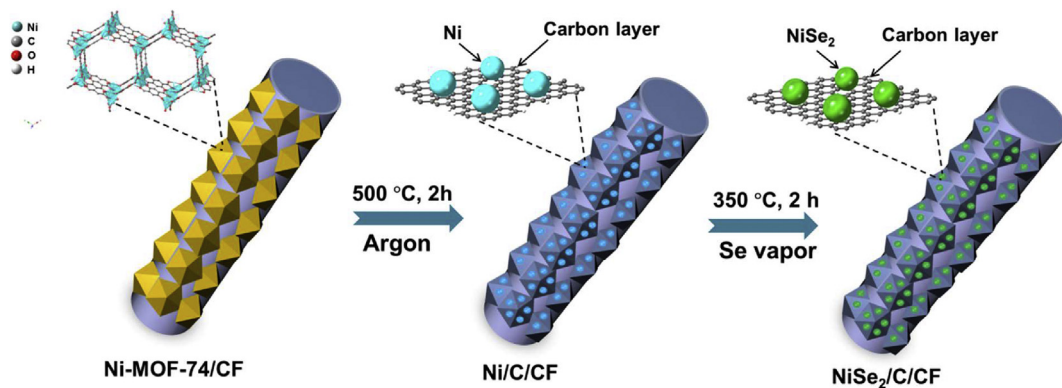


**Fig. 1 – Schematic illustration of the fabrication route of NiSe<sub>2</sub>/C/CF.**

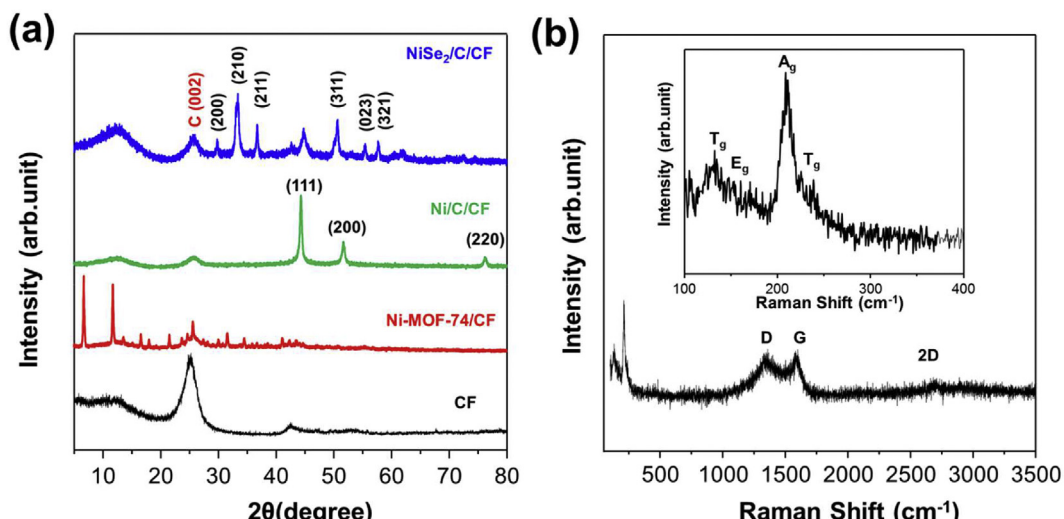


**Fig. 2 – (a) XRD patterns of CF, Ni-MOF-74/CF, Ni/C/CF, and NiSe<sub>2</sub>/C/CF. (b) Raman spectra of NiSe<sub>2</sub>/C/CF.**

**Fig. 3** exhibits the SEM images of the as-prepared of CF, Ni-MOF-74/CF, Ni/C/CF, and NiSe<sub>2</sub>/C/CF. CF treated by heat displays a flat surface with a diameter of 8–10 µm, as shown in **Fig. 3a** and b. As depicted in **Fig. 3c**, the Ni-MOF-74 crystals uniform cover on CF. Under high magnification, we can see that crystals were connected to create flower-shaped Ni-MOF-74 with a smooth surface (**Fig. 3d**). After annealed, Ni-MOF-74 converted into Ni nanoparticles embedded on carbon layers, as displayed in **Fig. 3e**. The surface of NiSe<sub>2</sub>/C/CF was also changed after selenization was conducted at 350 °C for 2 h (**Fig. 3f**). The TEM image (**Fig. 4a** and b) indicates that many NiSe<sub>2</sub> nanograins are distributed on carbon frameworks. For the purpose of d-space measurement, HRTEM were analyzed, as shown in **Fig. 4c**. The d-space is calculated to be 0.296 nm, which was assigned to the (200) facet. The structure of NiSe<sub>2</sub>/C/CF is further proved by EDS elemental mappings. As shown in **Fig. 4d**, the elements of Ni, Se and C are uniformly distributed on carbon matrix.

For chemical state analysis, XPS was adopted. **Fig. 5a** shows the survey spectrum of NiSe<sub>2</sub>/C/CF and implies the presence of Ni, Se, and C in the compound. As depicted in Ni 2p XPS spectra (**Fig. 5b**), two prominent peaks located at 853.3 (S1) and 870.6 eV (S1') are indexed to Ni<sup>2+</sup> 2p<sub>3/2</sub> and 2p<sub>1/2</sub>, respectively,

while the oxidation phase of Ni<sup>3+</sup> is identified at 855.9 eV (S2) and 873.9 eV (S2'). Also, two shakeup excitation of Ni<sup>2+</sup> was recorded at 861.1 eV (S3) and 880.0 eV (S3') [18,21]. For Se 3d XPS spectra (**Fig. 5c**), the binding energies of 55.4 eV and 54.5 eV are ascribed to the Se 3d<sub>5/2</sub> and Se 3d<sub>3/2</sub>. Also, the existence of a peak at 59.1 eV is suspected of the selenium oxides [23,49]. As depicted in **Fig. 5d**, C 1s can be devaluated to three peaks, which were assigned to 284.6 eV (C—C), 285.7 eV (C—O), and (287.3 eV (C=O).

The HER properties of the as-prepared working electrodes, including CF, Ni-MOF-74/CF, Ni/C/CF, and NiSe<sub>2</sub>/C/CF, were investigated in a three-electrode system with acidic sulfuric solution. **Fig. 6a** displays the polarization curves of CF, Ni-MOF-74/CF, Ni/C/CF, and NiSe<sub>2</sub>/C/CF and Pt/C. CF did not depict any catalytic activity for hydrogen evolving, whereas the Pt/C electrode depicts the best HER yield. Ni-MOF-74/CF gives a poor HER catalytic performance due to its containing organic component, which causes a high charge transfer resistance. However, when Ni-MOF-74/CF samples were annealed in Argon gas, Ni-MOF-74/CF was transformed into Ni nanoparticles anchored on the carbon layer (Ni/C/CF), which presents a good HER activity. Furthermore, after selenization, NiSe<sub>2</sub>/C/CF gives a better HER yield than the other working

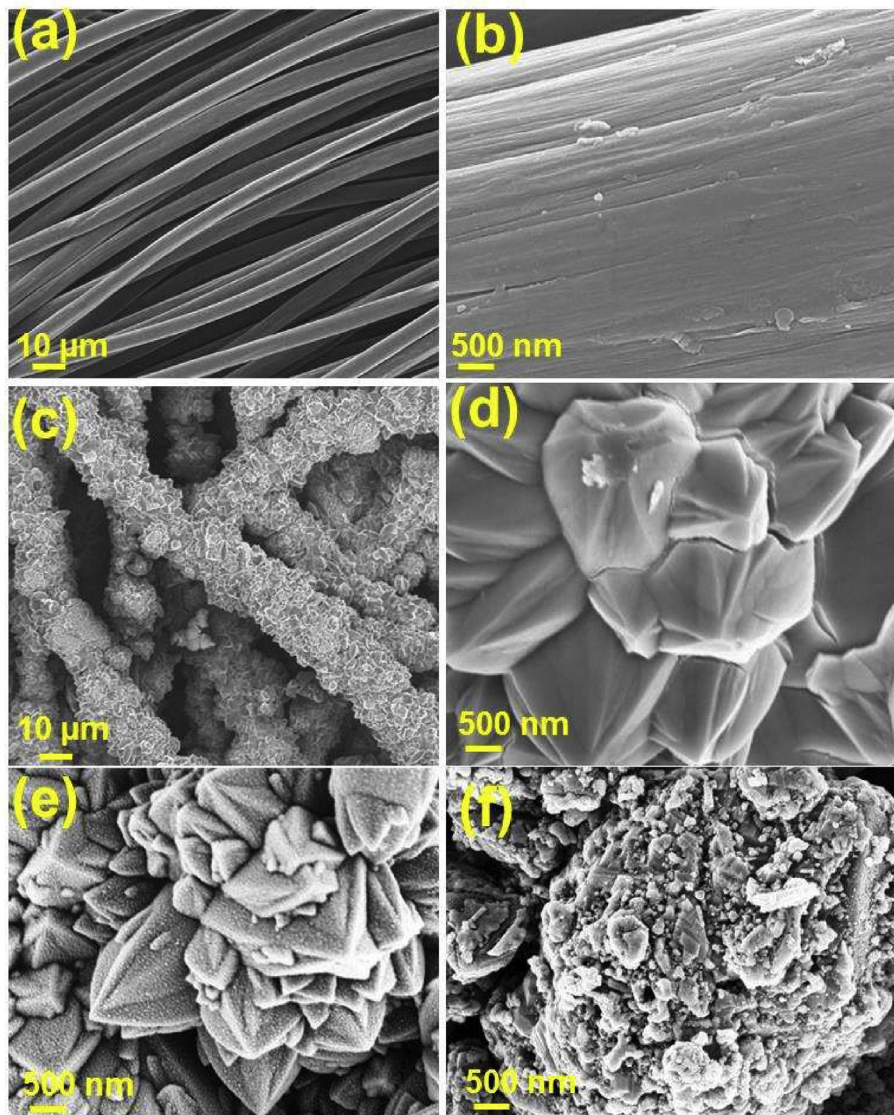


**Fig. 3 – SEM images of (a, b) CF, (c,d) Ni-MOF-74/CF, (e) Ni/C/CF and (f) NiSe<sub>2</sub>/C/CF.**

electrode. In particular, Tafel slope and overpotential at 10 mA/cm<sup>2</sup> were gathered from linear sweep voltammetry (LSV) measurements, as depicted in Fig. 6 b,c. NiSe<sub>2</sub>/C/CF electrode exhibits an overvoltage of 209 mV, which is smaller than that of Ni/C/CF (341 mV) and Ni-MOF-74/CF (475 mV). Also, the Tafel slope value of NiSe<sub>2</sub>/C/CF samples is 74.1 mV/dec, which is smaller than that of Ni/C/CF (95.6 mV per/dec) and Ni-MOF-74/CF (117.9 mV per/dec). Theoretically, The mechanism of hydrogen evolving under acidic condition involves two steps. Step 1 (Volmer reaction): proton was adsorbed on the catalyst surface ( $\text{H}_3\text{O}^{++} + \text{e}^- \rightarrow \text{H}_{\text{ads}} + \text{H}_2\text{O}$ ), which will generate a slope of ~120 mV/dec. Step 2 may take place two processes. The first process, called the Heyrovsky reaction, occurs the electrochemical desorption ( $\text{H}_3\text{O}^{++} + \text{H}_{\text{ads}} + \text{e}^- \rightarrow \text{H}_2 \uparrow + \text{H}_2\text{O}$ ), which creates a slope of ~40 mV/dec. The second process is called the Tafel reaction, exhibiting chemical desorption ( $\text{H}_{\text{ads}} + \text{H}_{\text{ads}} \rightarrow \text{H}_2$ ), producing a 30 mV/dec slope. Therefore, we propose that the HER mechanism of NiSe<sub>2</sub>/C/CF is the combination of the Volmer and Heyrovsky

reactions. The changes in HER catalytic performance of the working electrode can be assigned to electrochemically active surface area (ECSA) [50–52]. We thus conduct to determine ECSA, which is related to double-layer capacitances. CV measurements were carried out in a specific potential zone of 0.1–0.2 (V vs. RHE) at seven different scan rates (20–140 mV/s), which only contains non-faradaic current (Fig. S1). Fig. 6d shows the change of current density with scan rates, the slope of these plots is  $C_{dl}$ . NiSe<sub>2</sub>/C/CF gives a high  $C_{dl}$  value (12.5 mF/cm<sup>2</sup>) which is about two times and four times higher than Ni/C/CF (6.7 mF/cm<sup>2</sup>) and Ni-MOF-74 (2.9 mF/cm<sup>2</sup>). This finding proves that NiSe<sub>2</sub>/C/CF has the largest effective surface area, which indicates a strong relationship between ECSA and catalytic properties [53]. Impedance measurement was chosen to evaluate the reaction kinetic for hydrogen evolving. Fig. 6e depicts the Nyquist plots of Ni-MOF-74/CF, Ni/C/CF and NiSe<sub>2</sub>/C/CF. An equivalent circuit (the inset of Fig. 6e) shows two quasi-semicircles, revealing the porosity of MOF-derived materials [54]. Notably,  $R_s$ ,  $R_p$ , and  $R_{ct}$  is indexed to the series

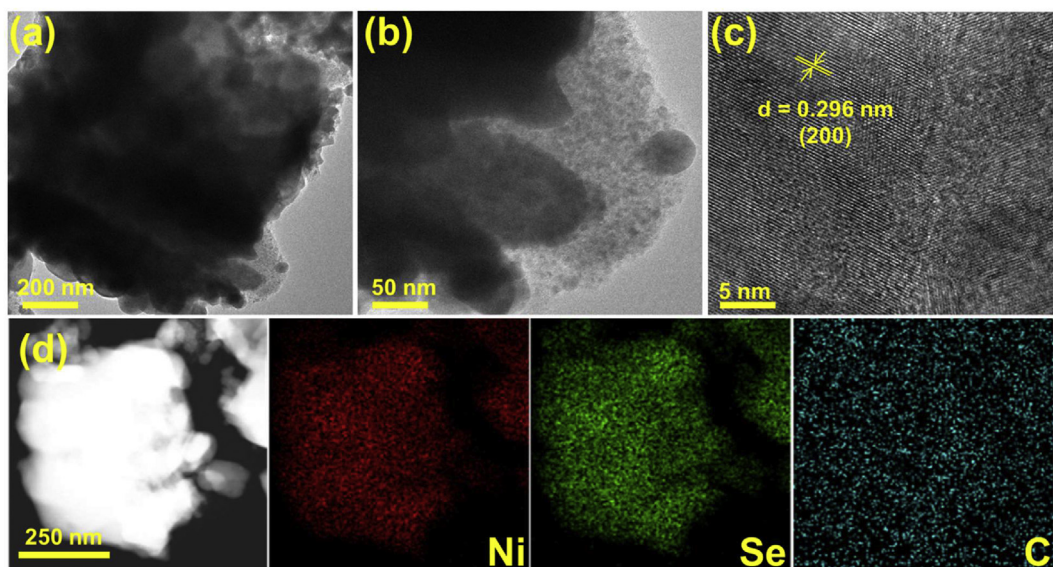


**Fig. 4 – (a, b) TEM images of NiSe<sub>2</sub>/C/CF. (c) HRTEM image of NiSe<sub>2</sub>/C/CF. (d) EDS elemental mapping images of NiSe<sub>2</sub>/C/CF.**

resistance, polarization resistance, and electron transfer resistance, respectively.  $R_{ct}$  value of NiSe<sub>2</sub>/C/CF is 9 Ω, which is lower than that of Ni-MOF-74/CF (62.5 Ω) and Ni/C/CF (14.4 Ω).

This indicates that the charge transfer process on NiSe<sub>2</sub>/C/CF sample is faster than the other electrode in hydrogen evolving.

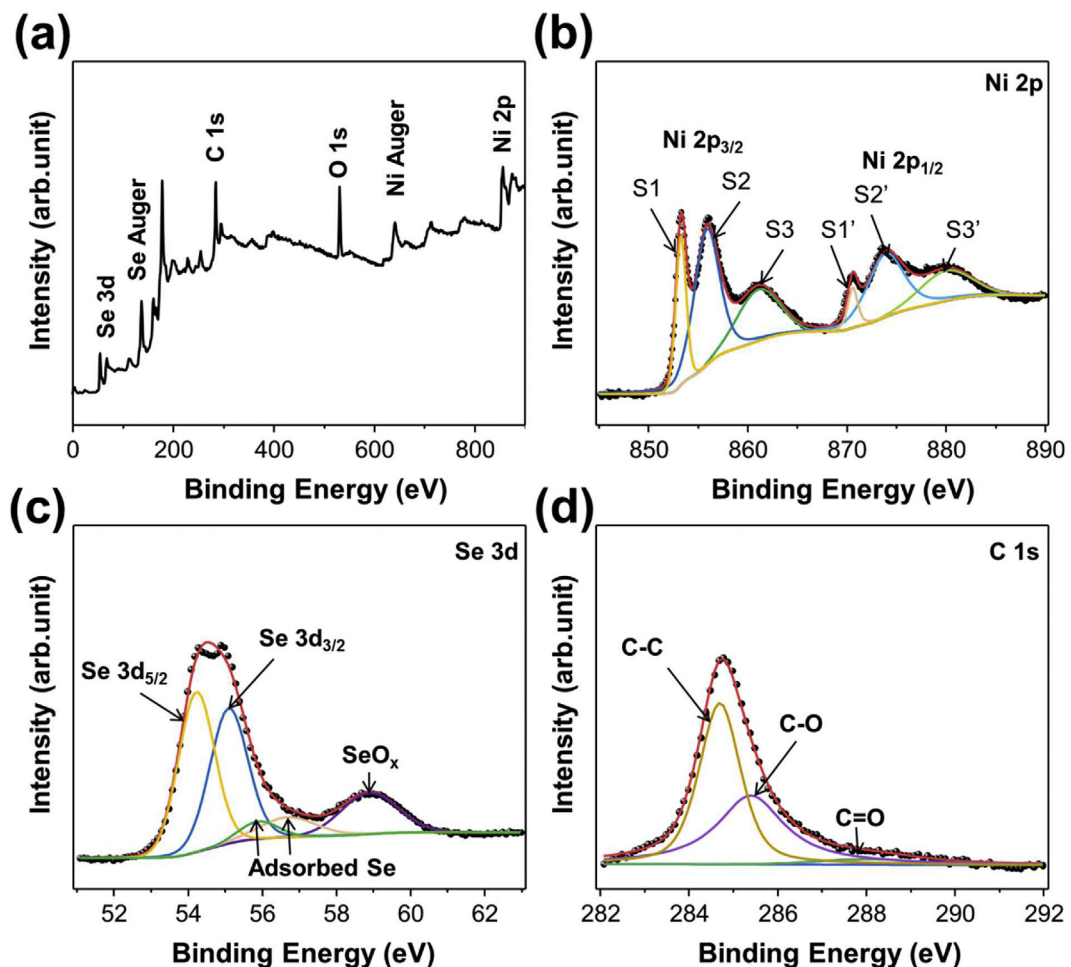


**Fig. 5 – XPS spectra of NiSe<sub>2</sub>/C/CF: (a) element survey, (b) Ni 2p, (c) Se 3, (d) C 1s.**

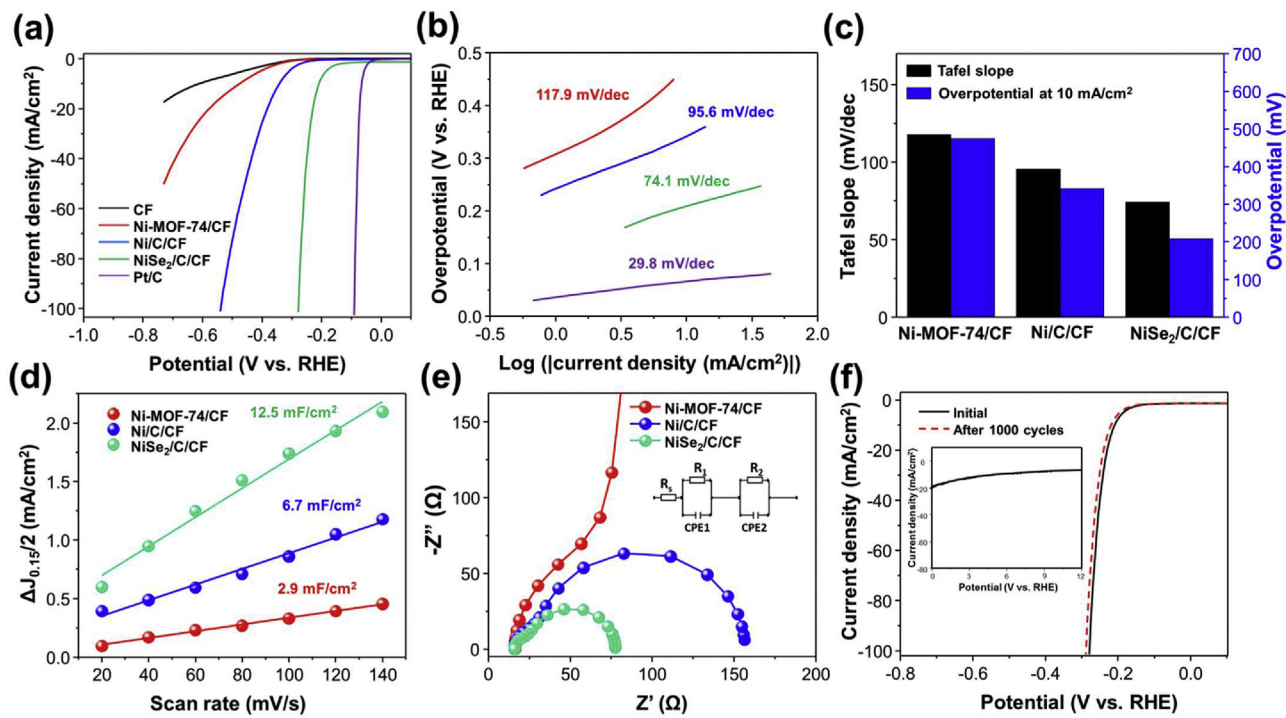


**Fig. 6 – (a)** Polarization curves in 0.5 M  $\text{H}_2\text{SO}_4$  **(b)** the corresponding Tafel slope. **(c)** Overpotential of as-prepared catalyst at 10  $\text{mA}/\text{cm}^2$ . **(d)** Estimated  $C_{dl}$  of Ni-MOF-74/CF, **(e)** Ni/C/CF and **(f)** NiSe<sub>2</sub>/C/CF. **(f)** Polarization curves of NiSe<sub>2</sub>/C/CF before and after 1000 CV cycles. Chronoamperometry test for NiSe<sub>2</sub>/C/CF at a constant voltage of 209 mV for 12 h.

For future commercial utilization, the stabilizing of electrocatalysts needs to be scrutinized in a long-term period. LSV of NiSe<sub>2</sub>/C/CF electrode after 1000 cycles is a slight change compare to the first cycles, as depicted in Fig. 6f. Furthermore, the durability of NiSe<sub>2</sub>/C/CF was examined at a specific voltage of 230 mV (vs. RHE) through a chronoamperometric analysis. The cathodic current density (20  $\text{mA}/\text{cm}^2$ ) of NiSe<sub>2</sub>/C/CF depicts an approximately 50% decrease in the HER activity after 12 h of hydrogen production (the inset of Fig. 6f). This outcome could be attributed to the consumption of protons and the impeding of the hydrogen bubble on the catalyst's surface [55–57]. After testing for the durability of NiSe<sub>2</sub>/C/CF, XRD and FE-SEM were analyzed to evaluate the crystal phase and morphological structure of the electrode. XRD pattern (Fig. S2a) reveals that the structure of NiSe<sub>2</sub>/C/CF built by NiSe<sub>2</sub> nanograins anchored carbon layer is unaltered. Besides, the FE-SEM image (Fig. S2b) of NiSe<sub>2</sub>/C/CF after 12 h of testing is identical before. This implies that NiSe<sub>2</sub>/C/CF is a durable electrode under acidic conditions for hydrogen production.

## Conclusion

The aim of this work is to design an economical electrocatalyst of NiSe<sub>2</sub> nanograins anchored Ni-MOF-derived porous carbon grown on carbon fiber (NiSe<sub>2</sub>/C/CF) and evaluate its catalytic activities for hydrogen production. This strategy gives emerging effects from NiSe<sub>2</sub> nanograins and 3D conductive substrate of CF, facilitating active species exposure and electron transport in the electrochemical HER

application. As a result, NiSe<sub>2</sub>/C/CF electrode displayed a good catalytic performance for hydrogen generation. In particular, NiSe<sub>2</sub>/C/CF only needs a small overvoltage of 209 mV to achieve a cathodic current density of 10  $\text{mA}/\text{cm}^2$ . Furthermore, this catalyst also maintains catalytic activity after 1000 cycles of testing in the acidic electrolyte. Although this study focuses on nickel diselenide, the findings may well have a bearing on the fabrication of transition metal compounds on CF from MOF precursors for the field of catalysis.

## Declaration of competing interest

The authors declare that they have no known competing financial interests or personal relationships that could have appeared to influence the work reported in this paper.

## Acknowledgments

This research was funded by Vietnam National Foundation for Science and Technology Development (NAFOSTED) under grant number 104.05-2020.15.

## Appendix A. Supplementary data

Supplementary data to this article can be found online at <https://doi.org/10.1016/j.ijhydene.2022.04.127>.

## REFERENCES

- [1] Yao N, Tan T, Yang F, Cheng G, Luo W. Well-aligned metal–organic framework array-derived  $\text{CoS}_2$  nanosheets toward robust electrochemical water splitting. *Mater Chem Front* 2018;2:1732–8.
- [2] Bai C, Wei S, Deng D, Lin X, Zheng M, Dong Q. A nitrogen-doped nano carbon dodecahedron with  $\text{Co}@\text{Co}_3\text{O}_4$  implants as a bi-functional electrocatalyst for efficient overall water splitting. *J Mater Chem* 2017;5:9533–6.
- [3] Yan X, Tian L, He M, Chen X. Three-dimensional crystalline/amorphous  $\text{Co}/\text{Co}_3\text{O}_4$  core/shell nanosheets as efficient electrocatalysts for the hydrogen evolution reaction. *Nano Lett* 2015;15:6015–21.
- [4] Paid AY, Barnett AO, Seland F, Sunde S. Ni/NiO nanosheets for alkaline hydrogen evolution reaction: in situ electrochemical-Raman study. *Electrochim Acta* 2020;361:137040.
- [5] Park SM, Jang MJ, Park YS, Lee J, Jeong J-y, Jung J, et al. Synthesis and characterization of the  $\text{Cu}_{0.72}\text{Co}_{2.28}\text{O}_4$  catalyst for oxygen evolution reaction in an anion exchange membrane water electrolyzer. *Korean J Met Mater* 2019;58:49–58.
- [6] Tekalgne MA, Van Nguyen K, Nguyen DLT, Nguyen V-H, Nguyen TP, Vo D-VN, et al. Hierarchical molybdenum disulfide on carbon nanotube-reduced graphene oxide composite paper as efficient catalysts for hydrogen evolution reaction. *J Alloys Compd* 2020;823:153897.
- [7] Hasani A, Van Le Q, Tekalgne M, Choi M-J, Lee TH, Jang HW, et al. Direct synthesis of two-dimensional  $\text{MoS}_2$  on p-type Si and application to solar hydrogen production. *NPG Asia Mater* 2019;11:1–9.
- [8] Hasani A, Van Le Q, Tekalgne M, Choi M-J, Choi S, Lee TH, et al. Fabrication of a  $\text{WS}_2/\text{p-Si}$  heterostructure photocathode using direct hybrid thermolysis. *ACS Appl Mater Interfaces* 2019;11:29910–6.
- [9] Nguyen TP, Kim SY, Lee TH, Jang HW, Van Le Q, Kim IT. Facile synthesis of  $\text{W}_2\text{C}@\text{WS}_2$  alloy nanoflowers and their hydrogen generation performance. *Appl Surf Sci* 2020;504:144389.
- [10] Zhao Y, Wang S, Liu H, Guo X, Zeng X, Wu W, et al. Porous  $\text{Mo}_2\text{C}$  nanorods as an efficient catalyst for the hydrogen evolution reaction. *J Phys Chem Solid* 2019;132:230–5.
- [11] Chen Z-Y, Duan L-F, Sheng T, Lin X, Chen Y-F, Chu Y-Q, et al. Dodecahedral  $\text{W}@\text{WC}$  composite as efficient catalyst for hydrogen evolution and Nitrobenzene reduction reactions. *ACS Appl Mater Interfaces* 2017;9:20594–602.
- [12] Lee C, Bang K, Hong D, Lee HM. Recent progress in first principle calculation and high-throughput screening of electrocatalysts: a review. *Korean J Met Mater* 2019;57:1–9.
- [13] Nguyen TP, Nguyen DMT, Le HK, Vo D-VN, Lam SS, Varma RS, et al. MXenes: applications in electrocatalytic, photocatalytic hydrogen evolution reaction and  $\text{CO}_2$  reduction. *Mol Catal* 2020;486:110850.
- [14] Nguyen TP, Nguyen DLT, Nguyen V-H, Le T-H, Ly QV, Vo D-VN, et al. Facile synthesis of  $\text{WS}_2$  hollow spheres and their hydrogen evolution reaction performance. *Appl Surf Sci* 2020;505:144574.
- [15] Guo W, Le QV, Do HH, Hasani A, Tekalgne M, Bae S-R, et al.  $\text{Ni}_3\text{Se}_4@\text{MoSe}_2$  composites for hydrogen evolution reaction. *Appl Sci* 2019;9:5035.
- [16] Kwon IS, Kwak IH, Debela TT, Abbas HG, Park YC, Ahn J-p, et al. Se-rich  $\text{MoSe}_2$  nanosheets and their superior electrocatalytic performance for hydrogen evolution reaction. *ACS Nano* 2020;14:6295–304.
- [17] Li J, Hong W, Jian C, Cai Q, He X, Liu W. High-performance hydrogen evolution at a  $\text{MoSe}_2-\text{Mo}_2\text{C}$  seamless heterojunction enabled by efficient charge transfer. *J Mater Chem* 2020;8:6692–8.
- [18] Li W, Yu B, Hu Y, Wang X, Yang D, Chen Y. Core–shell structure of  $\text{NiSe}_2$  nanoparticles@nitrogen-doped graphene for hydrogen evolution reaction in both acidic and alkaline media. *ACS Sustainable Chem Eng* 2019;7:4351–9.
- [19] Song D, Wang H, Wang X, Yu B, Chen Y.  $\text{NiSe}_2$  nanoparticles embedded in carbon nanowires as highly efficient and stable electrocatalyst for hydrogen evolution reaction. *Electrochim Acta* 2017;254:230–7.
- [20] Zhang J, Wang Y, Zhang C, Gao H, Lv L, Han L, et al. Self-supported porous  $\text{NiSe}_2$  nanowrinkles as efficient bifunctional electrocatalysts for overall water splitting. *ACS Sustainable Chem Eng* 2018;6:2231–9.
- [21] Yu B, Wang X, Qi F, Zheng B, He J, Lin J, et al. Self-assembled coral-like hierarchical architecture constructed by  $\text{NiSe}_2$  nanocrystals with comparable hydrogen-evolution performance of precious platinum catalyst. *ACS Appl Mater Interfaces* 2017;9:7154–9.
- [22] Liu T, Asiri AM, Sun X. Electrodeposited Co-doped  $\text{NiSe}_2$  nanoparticles film: a good electrocatalyst for efficient water splitting. *Nanoscale* 2016;8:3911–5.
- [23] Wang T, Gao D, Xiao W, Xi P, Xue D, Wang J. Transition-metal-doped  $\text{NiSe}_2$  nanosheets towards efficient hydrogen evolution reactions. *Nano Res* 2018;11:6051–61.
- [24] Chaudhari NK, Jin H, Kim B, Lee K. Nanostructured materials on 3D nickel foam as electrocatalysts for water splitting. *Nanoscale* 2017;9:12231–47.
- [25] Wang D, Xu Y, Guo X, Fu Z, Yang Z, Sun W. Nickel foam as conductive substrate enhanced low-crystallinity two-dimensional iron hydrogen phosphate for oxygen evolution reaction. *J Alloys Compd* 2021;870:159472.
- [26] Hu X, Tian X, Lin Y-W, Wang Z. Nickel foam and stainless steel mesh as electrocatalysts for hydrogen evolution reaction, oxygen evolution reaction and overall water splitting in alkaline media. *RSC Adv* 2019;9:31563–71.
- [27] Teng X, Wang J, Ji L, Lv Y, Chen Z. Ni nanotube array-based electrodes by electrochemical alloying and de-alloying for efficient water splitting. *Nanoscale* 2018;10:9276–85.
- [28] Yu F, Yao H, Wang B, Zhang K, Zhang Z, Xie L, et al. Nickel foam derived nitrogen doped nickel sulfide nanowires as an efficient electrocatalyst for the hydrogen evolution reaction. *Dalton Trans* 2018;47:9871–6.
- [29] Zhang H, Guo H, Ren J, Jin X, Li X, Song R. Synergistic engineering of morphology and electronic structure in constructing metal-organic framework-derived Ru doped cobalt-nickel oxide heterostructure towards efficient alkaline hydrogen evolution reaction. *Chem Eng J* 2021;426:131300.
- [30] Sangeetha D, Bhat DK, Kumar SS, Selvakumar M. Improving hydrogen evolution reaction and capacitive properties on  $\text{CoS}/\text{MoS}_2$  decorated carbon fibers. *Int J Hydrogen Energy* 2020;45:7788–800.
- [31] Wei L, Karahan HE, Zhai S, Yuan Y, Qian Q, Goh K, et al. Microbe-derived carbon materials for electrical energy storage and conversion. *J Energy Chem* 2016;25:191–8.
- [32] Ding Q, Liu M, Miao Y-E, Huang Y, Liu T. Electrospun nickel-decorated carbon nanofiber membranes as efficient electrocatalysts for hydrogen evolution reaction. *Electrochim Acta* 2015;159:1–7.
- [33] Liu H-J, Wang X-M, Cui W-J, Dou Y-Q, Zhao D-Y, Xia Y-Y. Highly ordered mesoporous carbon nanofiber arrays from a crab shell biological template and its application in supercapacitors and fuel cells. *J Mater Chem* 2010;20:4223–30.
- [34] Qu B, Yu X, Chen Y, Zhu C, Li C, Yin Z, et al. Ultrathin  $\text{MoSe}_2$  nanosheets decorated on carbon fiber cloth as binder-free

- and high-performance electrocatalyst for hydrogen evolution. *ACS Appl Mater Interfaces* 2015;7:14170–5.
- [35] Hou D, Zhou W, Liu X, Zhou K, Xie J, Li G, et al. Pt nanoparticles/MoS<sub>2</sub> nanosheets/carbon fibers as efficient catalyst for the hydrogen evolution reaction. *Electrochim Acta* 2015;166:26–31.
- [36] Zang X, Zhou C, Shao Q, Yu S, Qin Y, Lin X, et al. One-step synthesis of MoS<sub>2</sub> nanosheet arrays on 3D carbon fiber felts as a highly efficient catalyst for the hydrogen evolution reaction. *Energy Technol* 2019;7:1900052.
- [37] Zhang N, Gan S, Wu T, Ma W, Han D, Niu L. Growth control of MoS<sub>2</sub> nanosheets on carbon cloth for maximum active edges exposed: an excellent hydrogen evolution 3D cathode. *ACS Appl Mater Interfaces* 2015;7:12193–202.
- [38] Wang X, He J, Yu B, Sun B, Yang D, Zhang X, et al. CoSe<sub>2</sub> nanoparticles embedded MOF-derived Co-NC nanoflake arrays as efficient and stable electrocatalyst for hydrogen evolution reaction. *Appl Catal, B* 2019;258:117996.
- [39] Guan C, Liu X, Elshahawy AM, Zhang H, Wu H, Pennycook SJ, et al. Metal–organic framework derived hollow CoS<sub>2</sub> nanotube arrays: an efficient bifunctional electrocatalyst for overall water splitting. *Nanoscale Horiz* 2017;2:342–8.
- [40] Yan Y, Xia B, Li N, Xu Z, Fisher A, Wang X. Vertically oriented MoS<sub>2</sub> and WS<sub>2</sub> nanosheets directly grown on carbon cloth as efficient and stable 3-dimensional hydrogen-evolving cathodes. *J Mater Chem* 2015;3:131–5.
- [41] Hou CC, Zou L, Wang Y, Xu Q. MOF-Mediated fabrication of a porous 3D superstructure of carbon nanosheets decorated with ultrafine cobalt phosphide nanoparticles for efficient electrocatalysis and zinc–air batteries. *Angew Chem* 2020;132:21544–50.
- [42] Zhan J, Cao X, Zhou J, Xu G, Lei B, Wu M. Porous array with CoP nanoparticle modification derived from MOF grown on carbon cloth for effective alkaline hydrogen evolution. *Chem Eng J* 2021;416:128943.
- [43] Xie Z, Tang H, Wang Y. MOF-derived Ni-doped CoS<sub>2</sub> grown on carbon fiber paper for efficient oxygen evolution reaction. *Chemelectrochem* 2019;6:1206–12.
- [44] Dietzel PD, Panelia B, Hirscher M, Blom R, Fjellvåg H. Hydrogen adsorption in a nickel based coordination polymer with open metal sites in the cylindrical cavities of the desolvated framework. *Chem Commun* 2006:959–61.
- [45] Chen D-L, Shang H, Zhu W, Krishna R. Reprint of: transient breakthroughs of CO<sub>2</sub>/CH<sub>4</sub> and C<sub>3</sub>H<sub>6</sub>/C<sub>3</sub>H<sub>8</sub> mixtures in fixed beds packed with Ni-MOF-74. *Chem Eng Sci* 2015;124:109–17.
- [46] Zhao Z, Zuhra Z, Qin L, Zhou Y, Zhang L, Tang F, et al. Confinement of microporous MOF-74 (Ni) within mesoporous γ-Al<sub>2</sub>O<sub>3</sub> beads for excellent ultra-deep and selective adsorptive desulfurization performance. *Fuel Process Technol* 2018;176:276–82.
- [47] Yuan Q, Yu Y, Gong Y, Bi X. Three-dimensional N-doped carbon nanotube frameworks on Ni foam derived from a metal–organic framework as a bifunctional electrocatalyst for overall water splitting. *ACS Appl Mater Interfaces* 2019;12:3592–602.
- [48] Singh AK, Yasri N, Karan K, Roberts EP. Electrocatalytic activity of functionalized carbon paper electrodes and their correlation to the Fermi level derived from Raman spectra. *ACS Appl Energy Mater* 2019;2:2324–36.
- [49] Wang B, Wang Z, Wang X, Zheng B, Zhang W, Chen Y. Scalable synthesis of porous hollow CoSe<sub>2</sub>–MoSe<sub>2</sub>/carbon microspheres for highly efficient hydrogen evolution reaction in acidic and alkaline media. *J Mater Chem* 2018;6:12701–7.
- [50] Kong D, Wang H, Lu Z, Cui Y. CoSe<sub>2</sub> nanoparticles grown on carbon fiber paper: an efficient and stable electrocatalyst for hydrogen evolution reaction. *J Am Chem Soc* 2014;136:4897–900.
- [51] Zhang H, Li Y, Zhang G, Wan P, Xu T, Wu X, et al. Highly crystallized cubic cattierite CoS<sub>2</sub> for electrochemically hydrogen evolution over wide pH range from 0 to 14. *Electrochim Acta* 2014;148:170–4.
- [52] Chen Z, Cummins D, Reinecke BN, Clark E, Sunkara MK, Jaramillo TF. Core–shell MoO<sub>3</sub>–MoS<sub>2</sub> nanowires for hydrogen evolution: a functional design for electrocatalytic materials. *Nano Lett* 2011;11:4168–75.
- [53] Faber MS, Dziedzic R, Lukowski MA, Kaiser NS, Ding Q, Jin S. High-performance electrocatalysis using metallic cobalt pyrite (CoS<sub>2</sub>) micro-and nanostructures. *J Am Chem Soc* 2014;136:10053–61.
- [54] Bhowmik T, Kundu MK, Barman S. Palladium nanoparticle–graphitic carbon nitride porous synergistic catalyst for hydrogen evolution/oxidation reactions over a broad range of pH and correlation of its catalytic activity with measured hydrogen binding energy. *ACS Catal* 2016;6:1929–41.
- [55] Xie J, Zhang H, Li S, Wang R, Sun X, Zhou M, et al. Defect-rich MoS<sub>2</sub> ultrathin nanosheets with additional active edge sites for enhanced electrocatalytic hydrogen evolution. *Adv Mater* 2013;25:5807–13.
- [56] Li S, Zhao L, Lei S, Liu A, Chen J, Li C, et al. Improved charge injection of edge aligned MoS<sub>2</sub>/MoO<sub>2</sub> hybrid nanosheets for highly robust and efficient electrocatalysis of H<sub>2</sub> production. *Nanoscale* 2020;12:5003–13.
- [57] Vikraman D, Hussain S, Akbar K, Truong L, Kathalingam A, Chun S-H, et al. Improved hydrogen evolution reaction performance using MoS<sub>2</sub>–WS<sub>2</sub> heterostructures by physicochemical process. *ACS Sustainable Chem Eng* 2018;6:8400–9.